Nature of the surface chemical bond in N_2 on Ni(100) studied by x-ray-emission spectroscopy and *ab initio* calculations

P. Bennich, T. Wiell, O. Karis, M. Weinelt, N. Wassdahl, and A. Nilsson
Department of Physics, Uppsala University, Box 530, S-751 21 Uppsala, Sweden

M. Nyberg and L. G. M. Pettersson
FYSIKUM, University of Stockholm, Box 6730, S-113 85 Stockholm, Sweden

J. Stöhr and M. Samant
IBM Research Division, Almaden Research Center, 650 Harry Road, San Jose, California 95120-6099
(Received 17 June 1997)

The electronic structure of the system N_2/Ni(100) has been studied by means of angle-resolved x-ray-emission spectroscopy (XES) and *ab initio* calculations. XES allows a symmetry-resolved decomposition of the $2p$ density of states projected on each N atom. The calculations reproduce the experimental spectra well. Our results show that it is necessary to use an atom-specific description rather than treating the molecule and substrate as separate units. Hence a model of the surface chemical bond for this system is presented, in which the N_2 1π–Ni $3d$ interaction is important for the bond of N_2 to the Ni(100) surface. The weakening of the internal π is seen as the appearance of a nonbonding orbital whose character is essentially Ni $3d$ with a contribution of N $2p$ lone pair on the outer nitrogen atom. The σ system strongly polarizes in order to minimize the Pauli repulsion with the Ni $4sp$ states in the substrate. The traditional picture of the Blyholder model, which in a frontier orbital framework involves σ donation and π backdonation with more or less unperturbed orbitals, is not in agreement with the experimental data and is not supported by the calculations. In order to create the adsorbate orbitals we need to involve the whole original π system of the free molecule, i.e., both the 1π and $2\pi^*$ orbitals. [S0163-1829(98)04415-4]

I. INTRODUCTION

A recurrent theme in surface science concerns the understanding of the chemical bond between an adsorbed molecule and a metal surface. The central task is to achieve a proper description of the electronic structure of the molecule and substrate, and the changes that occur in the electronic levels upon bond formation. From numerous experimental and theoretical efforts, different models have emerged where the gross features most often are described in terms of an interaction between ''frontier orbitals'' localized on the molecule, and the metal electronic levels, such as the sp and d bands. Conceptually, frontier orbitals means that it is sufficient to focus on the highest occupied and lowest unoccupied molecular orbitals (MO's) of the free molecule which interact with the substrate.

However, a different approach is to start from the *atomic* orbitals, using a linear combination of atomic orbitals description of the electronic levels. The advantage is a more detailed picture but at the expense of increased complexity. From a theoretical point of view such an approach is rather straightforward. However, in the past this has not been an easy path on the experimental side. For example, probes like ultraviolet photoemission spectroscopy (UPS), which is one of the most common techniques for probing the valence levels, do not allow a separation in terms of atomic contributions to the electronic levels. On the other hand, x-ray-emission spectroscopy (XES), applied to adsorbate systems, has in recent years[1–6] been shown to be a spectroscopy well suited for obtaining atom-specific electronic structure information due to the localization of the core-excited intermediate state. Furthermore, angle-dependent measurements make it possible to separate states of different molecular symmetry.

In the case of XES applied to the N_2/Ni(100) system, the emission from transitions of $2p \rightarrow 1s$ type is measured. This means that spectra related to the $2p$ contribution to the valence states are obtained. We have furthermore used the fact that the chemical shift between the two N atoms is large enough to allow a separation of the valence states on each atom. Since the adsorbate system is oriented, we have also been able to determine the σ and π symmetries of the observed states. Due to the orientation of the molecule and the selection rules governing the XE process, it follows[7] that, in normal emission, orbitals with pure π symmetry can be observed, and in grazing emission both π and σ orbitals are probed.

From a theoretical point of view XE spectroscopy provides a very strong basis for the evaluation of methods for population analysis. Many different schemes for subdividing the charge density into different types of contributions assigned to the respective centers have been proposed, but the lack of a means to measure the atomic populations directly has made all techniques somewhat arbitrary and a matter of taste. Since the XE process, for a $1s$ initial core hole, relies on the projection of the local p character onto the spatially well-localized core orbital, this in effect provides exactly such a tool to analyze and decompose the charge density into separate atomic contributions. However, for a complete un-

derstanding it is important also to consider the effects due to the core hole in the intermediate state. Recent theoretical model calculations of the XE process in adsorbates give no significant modification of the interpretation using ground-state frozen orbitals or a fully relaxed core-hole state.[8] There are small changes of the relative intensities except for a strong state close to the Fermi level appearing in the fully relaxed core-hole state calculation. The large transition intensity for this state is not seen in experiments, and could be an artifact of the theoretical model. We should bear in mind that the states close to the Fermi level could get somewhat enhanced intensity through the metallic screening in the core-hole state.

The N_2/Ni(100) system has, together with the much more studied system CO/Ni(100), served as a prototype system for molecular adsorption in general. The most common description of the surface chemical bond in these systems is the so-called Blyholder model[9] which is based on the frontier orbital concept. This model describes the bonding in terms of 5σ donation into the substrate and a backdonation into the $2\pi^\star$. However, our results show that such a model for N_2/Ni(100) does not provide a correct description of the bonding, and that an atomic-orbital based picture is necessary in order to describe and explain the observed spectral distributions. A short communication of the experimental results was published recently.[5] In the present paper we describe the experiment in more detail, and compare the results with *ab initio* calculations on a N_2/Ni_{13} cluster. The experimental and calculated results are mutually consistent, and lead to a more detailed and somewhat modified picture compared to the one previously presented.[5]

The paper is organized as follows: after this introduction, Sec. II discusses previous experimental and theoretical studies. Experimental and computational details are given in Secs. III and IV, respectively. The XES and calculated results are presented in Sec. V, whereas the discussion and summary are found in Secs. VI and VII, respectively.

II. PREVIOUS RESULTS ON N_2/NI(100)

N_2 is a homonuclear molecule with electronic states that are evenly distributed on each atom. N_2 is isoelectronic with CO, and the valence levels are, using $C_{\infty v}$ notation as for CO, the 3σ, 4σ, 1π, 5σ (highest occupied level), and $2\pi^\star$ (lowest unoccupied level). When chemisorbed on a Ni(100) surface, the molecular axis has been found in a perpendicular geometry relative to the surface plane.[10,11] This is also the adsorption geometry for CO adsorbed on Ni(100),[12,13] but the chemisorption strength of N_2/Ni(100) is much weaker than for CO/Ni(100) [0.5 (Ref. 14) and 1.4 eV,[15] respectively].

The results from UPS measurements[16,17] are complex due to the presence of multielectron states in the spectra (the creation of x-ray decay satellites is much less probable, since no electron is removed from the system). In terms of screened one-electron states it was, however, concluded in Ref. 16 that the 5σ and 1π levels coincide at 7.6 eV and that the 4σ level is found at 12.4 eV. An interesting point when compared to CO/Ni(100), also studied in that paper,[16] was that the relative shift between the 5σ and 4σ levels *increased* from the gas-phase values, as opposed to the case for CO/Ni(100) where it instead decreased. A similar behavior was found for N_2/Ni(110), studied in Ref. 17.

Furthermore, although partial occupation of the $2\pi^\star$ level would be probable for N_2/Ni(100), in line with observations for CO/Ni(100),[18] no such evidence was found. However, the strong and overlapping Ni $3d$ band makes it very difficult to make such observations, and the authors of Ref. 16 only concluded that their data were not conclusive on this matter.

In conjunction with the UPS measurements in Ref. 16, Hartree-Fock calculations on linear NiN_2, as a model of chemisorption on the Ni(100) surface, were also made and presented in Ref. 19. Among other properties, the atomic contributions to the wave functions, of relevance for the present study, were calculated. Starting with the σ system, it was found that the 3σ level was slightly polarized towards the outer N atom compared to the gas-phase s and p atomic contributions; that the 4σ level clearly polarized toward the inner N atom; and that the 5σ level also clearly polarized toward the outer N atom. No Ni contributions at all were seen in the 3σ level. Although the Ni contributions to the 4σ and 5σ levels were small, a significant Ni-N_2 overlap population between the Ni and inner N atoms was found for both levels, meaning that they equally contribute to the Ni-N_2 bond. The Ni σ orbitals ($3d_\sigma$ and $4sp_\sigma$) were described as antibonding with the N_2, thus reducing the bonding in the σ space.

Moving next to the π system, two occupied π levels were found: 1π- and Ni $3d_\pi$-derived levels. The 1π level was found to be slightly polarized toward the inner N atom and with small Ni contributions, whereas the Ni $3d_\pi$ level was found to be dominated completely by the Ni atom, but with some contribution from the outer N atom (lone pair). However, the overlap population for both of these levels was practically zero and the binding energy for the whole molecule was only 0.1 eV, well below the experimental value of 0.5 eV (Ref. 14) for N_2/Ni(100).

Therefore, a model was set up, now with N_2 interacting with an excited Ni atom to model the interaction with the $4sp$ band: by occupying the Ni $4p_\pi$ orbital the possibility of an Ni $4sp$–N_2 $2\pi^\star$ interaction opens up. The results were in general agreement with the previous model, with the exception of an occupied π state made up by p orbitals distributed on all three atoms. The overlap population for this state was, furthermore, large, and the binding energy of the cluster increased substantially up to 1.13 eV. Thus the authors concluded that Ni $4sp$ donation to the empty N_2 $2\pi^\star$ is far more important than Ni $3d$ donation, and suggested that this should also be the case for the real situation [N_2/Ni(100)].

This picture is thus somewhat different compared to the Blyholder model for CO adsorption: since the spatial distribution for the π and σ systems are different for the two molecules, both the 4σ and 5σ levels are involved in the bonding for N_2, as opposed to CO, where only the 5σ level is involved. Furthermore, the Ni-to-N_2 backdonation is accomplished via the Ni $4sp$ bands, not the $3d$ band. Nevertheless, this picture is still in line with a donation–backdonation scheme, in which the backdonation into the empty N_2 $2\pi^\star$ makes the most important contribution to the bond. In Ref. 17 the interpretation of the experimental data in conjunction with theoretical calculations (Hartree-Fock,

X_α scattered wave and many-body Green's-function techniques) was again in terms of a σ-donation – π-backdonation scheme, but assigning the main bonding contributions to the σ interaction.

For the gas-phase linear NiN_2 system,[20,21] as well as for the corresponding NiCO molecule,[22] it was later shown that the self-consistent-field (SCF) level is insufficient to describe the bonding and reliably, more advanced multiconfigurational wave functions must be considered. The repulsion felt by the 4σ and 5σ orbitals against the $4s$ of the metal can be alleviated very efficiently by allowing for an s-d hybridization,[20] which requires a singlet-coupled Ni d^9s^1 atomic configuration and unequal occupations in the two hybrids; the ground state at this level of theory then becomes the $^1\Sigma^+$ state. A somewhat different interpretation was reached by Kao and Messmer,[21] who viewed the results rather in terms of involvement of the Ni d (Ref. 10) atomic configuration. Using generalized valence-bond configuration-interaction calculations, the $^1\Sigma^+$ ground-state was found with a shorter bonding distance (1.8 Å instead of 2.2 Å for the $^3\Delta$ from Ref. 16). The calculations were interpreted within the traditional picture of the σ-donation–π-backdonation scheme; however, the authors of this work favored a donation from the Ni $3d$ band rather than from the Ni $4sp$ band.

It should be realized that the previous calculations to some extent had different objectives: to model N_2 chemisorption in an on-top site and to describe the linear Ni-N_2 molecule in the gas phase. In the present work we will specifically discuss the N_2 interaction with the surface represented by cluster models, and we find best agreement with the earlier study of Brundle *et al.*[16] in terms of the character of the specific molecular orbitals and the polarization effects in the σ space. However, by also including several higher levels of calculation in combination with our experiments, we are able to draw more far-reaching, and different, conclusions for the π system, as will be evident later on.

III. EXPERIMENT

The experiment was performed at the Advanced Light Source, Berkeley, using the undulator beamline 8.0 which is equipped with a spherical grating monochromator of ''Dragon'' type. The resolution of the exciting radiation was set to 0.4 eV. The end station contains an electron energy analyzer (Scienta-200), a multichannel plate for x-ray-absorption measurements and an XE spectrometer. All instruments are mounted on an analysis chamber which can rotate around an axis parallel to the incoming beam.

The nickel crystal was mounted on a manipulator rod which was parallel to the incoming beam, i.e., the axis of rotation for the analysis chamber. In order to obtain high surface sensitivity, the incoming light was impinging on the surface at grazing angles of around $3°-5°$. The beam was focused to a spot size of 100×200 μm at the sample position. This yields an estimated photon flux of about 10^{13}–10^{14} photons per second within this area. The high flux is necessary in the XES experiments since the overall photon yield is of the order of 1:10.[11] In order to avoid radiation damage of the overlayer during the XE measurements, caused by the high flux of the incoming light, the spectra were collected by scanning the sample in front of the spectrometer entrance slit.

The XE spectrometer is based on a grazing incidence grating in combination with a movable multichannel detector;[23] the grating used for the N spectra has a radius of 5 m, and a groove density of 1200 lines/mm. The resolution was around 0.5 eV in the XE spectra. Photoemission measurements of the Ni Fermi edge were used to calibrate the photon energies. A $c(2\times2)$ overlayer of N_2/Ni(100) was prepared by a 10-L dose at temperatures below 110 K,[24] as confirmed by photoemission and low-energy electron-diffraction measurements.

IV. COMPUTATIONAL

The calculations have been performed for N_2 chemisorbed on-top on a 13-atom nickel cluster. The directly interacting central nickel atom was described including all electrons, while the surrounding 12 atoms were described as one-electron atoms, treating only the $4sp$ electrons explicitly. For this structure the Ni-N and internal N-N distances were optimized, and the wave function analyzed. Spectra were generated either approximately using the p populations on each nitrogen in the different molecular orbitals or by an explicit calculation of transition intensities in the deexcitation process using a frozen orbital approximation, i.e., the ground-state orbitals were used to represent both initial and final states. Calculations were also performed for the fully relaxed initial core-hole state, but led to an artificially high intensity from screening states at the Fermi level. The origin of this effect is not quite understood, but most likely due to an imbalance in the treatment of initial and final state relaxation effects. Earlier work on CO/Cu(100) (Ref. 8) has shown that, except for the region around the Fermi level, the frozen and relaxed orbital results show good agreement. The frozen-orbital description of the XE spectra seems to give the best overall agreement, and will thus be used in the present work to calibrate the intensities in the spectra generated from the populations.

The calculations have been performed in C_{2v} symmetry at several different levels of theory, including Hartree-Fock SCF, complete active space SCF (CASSCF) multireference average coupled pair functional, and density-functional theory (DFT). The interaction of N_2 with a single Ni atom was studied previously,[20] and the interaction was found to be dependent on a reduction of the σ repulsion through an s–d hybridization. This is dependent on having a d^9s^1 (^1D) electronic configuration on the Ni atom, and results in the formation of two, differently occupied, hybrid orbitals. This process requires that the $3d_\sigma$ and $4s$ orbitals are taken as active in the CASSCF calculation, and this was thus also done in the present study. On the cluster there are additional possibilities to reduce the σ repulsion, since the $4s$ may simply polarize onto surrounding cluster atoms. This possibility is also included by this choice of active orbitals for the σ symmetry. In order to allow $3d_\pi$ interaction with the N_2 $\pi^\star$, these two orbitals were furthermore taken to be active giving a rather compact description with six active electrons in six active orbitals. In the multireference calculations either 32 (full valence) or 24 electrons were correlated and two different treatments were made: either the dynamical

correlation space was reduced by retaining as reference only those configurations that describe the π interaction or by reducing the number of electrons in the correlation treatment by excluding the $3d_\delta$ orbitals together with two cluster orbitals (one in a_2, and one, well-localized, δ-type orbital in the a_1 symmetry).

The basis sets used were a $(10s5p2d)/[4s3p2d]$ basis in a general contraction[25] for nitrogen and the Wachters $(14s11p6d3f)/[5s4p3d1f]$ basis set for nickel.[26] The remaining nickel atoms in the cluster were described using a one-electron effective core potential (ECP) description in combination with a $(4s1p)/[2s1p]$ basis set. The one-electron ECP was developed by Panas, Siegbahn, and Wahlgren,[27] and has been tested on a number of systems.[28]

The DFT calculations were performed using the deMon code[29,30] on N_2 chemisorbed ontop of a pyramidal Ni_5 cluster assuming an overall singlet spin state. The choice of spin state leads to a spin-contaminated solution, but with the open-shell orbitals localized only on the cluster. Thus it was assumed that the spin contamination should not affect the qualitative results for the Ni-N_2 interaction. In these calculations all Ni atoms were treated at the all-electron level with the purpose of studying effects of a better representation of the Ni $3d$ band structure. Nitrogen was described using a triple-ζ plus polarization basis set while the nickel atoms were described using the SDZC basis[31] extended with two diffuse p functions and a diffuse d function. Gradient-corrected functionals[32] were used throughout and the N_2 chemisorption geometry was optimized for fixed Ni-cluster geometry.

The full spectrum calculations were performed using the direct SCF program DISCO,[33] which has recently been extended to treat x-ray-absorption[34] (XA) and x-ray-emission spectra.[8] In this approach to XES the nonorthogonal transition moments are normally computed between the fully relaxed core-hole state and the final state, which is represented by the ground-state orbitals. Thus final-state relaxation effects are assumed to be small compared with the relaxation of the core hole, and are thus neglected. Alternatively, the ground-state orbitals may be taken to represent both the initial core-hole state and the final state in a frozen-orbital picture; this approach was used in the present work. The valence binding energies are taken as the Koopmans values. This approach is only implemented for the Hartree-Fock calculation, and was thus only applied to a simpler closed-shell SCF wavefunction that approximated the above-described CASSCF calculation. The XES spectra from the CASSCF wave function were instead qualitatively generated by using the one-center approximation, and assigning intensities according to the amount of local p character as given by a Mulliken population analysis. It is realized that this type of charge partitioning is not unique, and that some uncertainty in the populations assigned to each center exists. However, this uncertainty is smaller for a homonuclear system such as N_2, and we furthermore believe that the changes in local orbital character upon adsorption should be more accurately represented. The peak positions were thus assigned according to the orbital energies for the corresponding orbitals in the closed-shell SCF calculation. In order to facilitate the comparison with the experimental spectra, the lines were convoluted with a Gaussian of 1.0 eV full width at half maximum (FWHM).

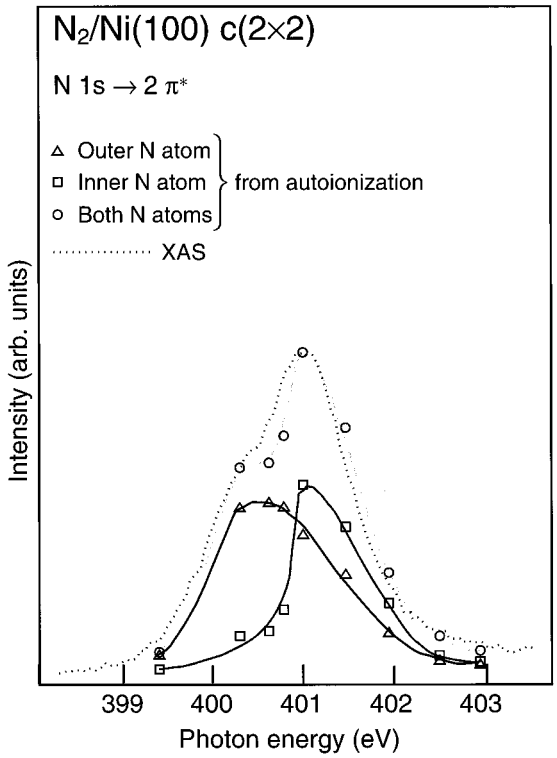

FIG. 1. X-ray-emission raw spectra. The upper panel displays spectra recorded for an excitation energy of 400.3 eV, yielding contributions from the outer N atom only; and the lower panel shows spectra recorded with an excitation energy of 401.5 eV, yielding contributions from both atoms.

V. RESULTS

A. X-ray-emission spectra

Treating x-ray emission as a two-step process, the first step is the creation of a core hole by an electron transition from a core level to either a bound, empty valence level or to the ionization continuum followed by, in a second step, the filling of the core hole by an electron from an occupied valence level under emission of x rays. It is of vital importance to use threshold excitation in the first step in order to avoid multiply excited states, since they can give rise to satellites in the XE spectra which would make the assignment of the ''one-electron'' states more difficult. Therefore, we always excited an N $1s$ electron into the lowest unoccupied $\pi^\star$ level.

Figure 1 shows the XA spectrum (dotted line) of N_2/Ni(100), taken from Ref. 35. By means of a decomposition based on autoionization spectra, the individual XA spectra for each nitrogen atom were obtained (solid line). The position of the N $1s \rightarrow 2\pi^\star$ resonance is estimated to 400.6 and 401.0 eV for the outer and inner N atoms, respectively. We choose energies close to these values when creating the initial state in the XE process: by exciting with a photon energy of 400.3 eV, only the outer atom contributed to the XE spectra; and by exciting with 401.5 eV, both atoms contributed but with a dominating contribution from the inner

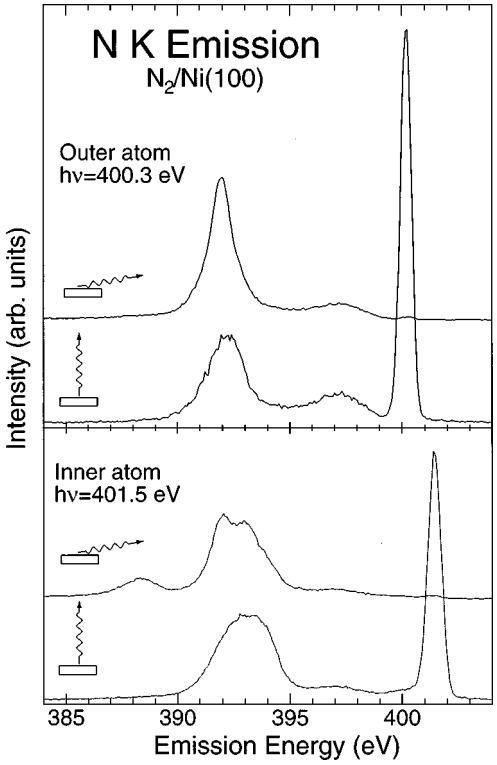

FIG. 2. X-ray-emission raw spectra. The upper panel displays spectra recorded for an excitation energy of 400.3 eV, yielding contributions from the outer N atom only; and the lower panel shows spectra recorded with an excitation energy of 401.5 eV, yielding contributions from both atoms.

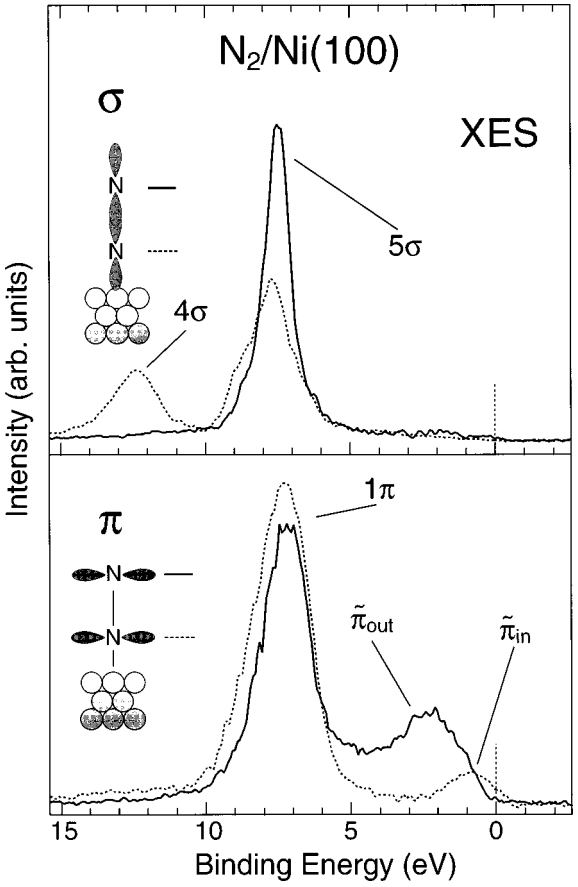

FIG. 3. Decomposed XE spectra in terms of symmetry and atomic site: the upper panel displays states of σ symmetry, and the lower panel states of π symmetry. The energy region is confined to the outer valence level. π states arising from the surface chemical bond are indicated with a tilde symbol.

atom. For each photon energy, a spectrum was recorded in a grazing and a normal emission geometry by rotating the x-ray spectrometer with the E vector of the incoming light fixed parallel to the surface.

The spectra recorded in this way are shown in Fig. 2. The energy scale refers to the emitted photon energy as recorded by the XE spectrometer, and the icons indicate the emission geometry. The intensities are scaled in an arbitrary way. The upper part of Fig. 2 displays the spectra recorded at 400.3-eV excitation energy, which are associated with the outer N atom only. Going from right (high energy) to left, the first feature, dominating in the normal-emission spectrum but also present in the grazing emission spectrum, occurs at 400.3 eV and is simply due to photons which are elastically scattered by the overlayer into the XE spectrometer. In the lower part of Fig. 2, the spectra for 401.5-eV excitation energy are displayed. The feature at 401.5 eV is again due to scattered photons. If we compare the remaining features with the 400.3-eV spectra, it is immediately seen that there are some differences. As the 401.5-eV spectra contain contributions from both atoms, it follows that the new features are associated with the inner atom. To be more specific, the relative amount from each atom will depend on the relative cross sections for exciting each of them at this particular photon energy. This in turn is given by the XA spectrum, and we will therefore use Fig. 1 again in order to separate the XE spectra, so that the ''pure'' spectra associated with the inner N atom can be obtained. We remark at this stage that there are no contributions from core-hole shake-up satellites in the 401.5-eV spectra, that could possibly have been created since the excitation energy is above threshold (400.3 eV): the excess energy of 1.2 eV is not enough to create any multiply excited states in the XE initial state.[24]

Figures 3 and 4 displays separated spectra which were obtained in three steps: first, the 400.3-eV spectra were subtracted from the 401.5-eV spectra after the relative intensities were set according to the XA spectrum in Fig. 1, thereby yielding ''pure'' inner N atom spectra; second, the contribution from scattered photons was subtracted with a modeled peak of Gaussian shape; and third, the pure σ spectra were obtained by subtracting the normal-emission spectra (containing only π states) from the grazing emission spectra ($\pi+\sigma$), using an intensity ratio of about 1:2 [π:($\pi+\sigma$)] for the outer atom, and 1:3 for the inner atom. These ratios are not known *a priori*, but resulted from the subtraction procedure where a criterion based on that the background levels should be similar after a subtraction was used.

For metallic systems, such as chemisorbed molecules, the position of the Fermi level is obtained from the corresponding core-level binding energy.[36] The spectra were thus put on a common binding-energy scale, obtained by subtracting the core-level photoemission binding energies of the two N atoms[24] [N(1s) outer atom: 399.4 eV; inner: 400.7 eV]. The figures are divided in an upper part, displaying states of σ symmetry, and a lower part, displaying states of π symmetry.

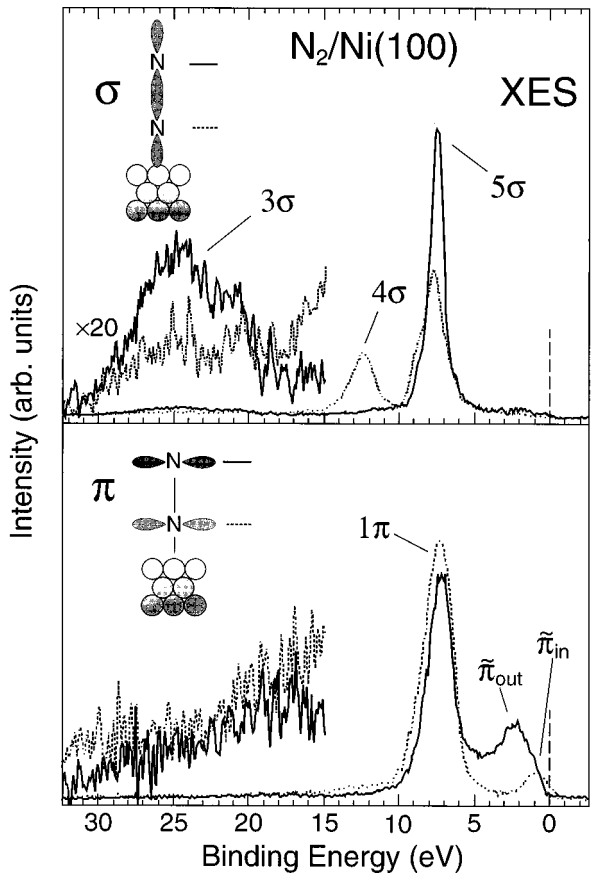

FIG. 4. Decomposed XE spectra in terms of symmetry and atomic site: the upper panel displays states of σ symmetry, and the lower panel states of π symmetry. The energy region is extended to include the inner valence region.

From the symmetry and the binding energies of the spectral features, it is straightforward to assign all features above 5 eV in analogy with UPS measurements.[16,17] All spectral peaks exhibit different intensities or shapes for the inner and outer N atoms. Even the 3σ state shows an intensity difference for the two atoms. Other interesting findings are the localization of the 4σ state to the inner N atom, with no visible spectral intensity from the outer N atom, and the larger 5σ localization to the outer N atom. Near the Fermi level we find molecular states of π symmetry which cannot be assigned based on the molecular orbitals of the free molecule. The state located on the outer N atom is centered at about 2.5-eV binding energy, while the state located on the inner N atom is centered at about 1 eV denoted $\tilde{\pi}_{\mathrm{out}}$ and $\tilde{\pi}_{\mathrm{in}}$, respectively.

There are a few structures in the separated spectra which probably can be attributed to artifacts in the subtraction procedure. There is some weak intensity in the outer atom σ symmetry spectra around 2 eV. The outer atom has a peak at 2.5 eV in the π spectrum, which might yield some remaining intensity in the σ spectrum. There is a shoulder on the inner nitrogen 5σ peak which we cannot assume to be real. The inner nitrogen σ symmetry spectrum involves two subtractions, and the shoulder appears in an emission energy region involving both the 1π and 5σ peaks on the outer atom.

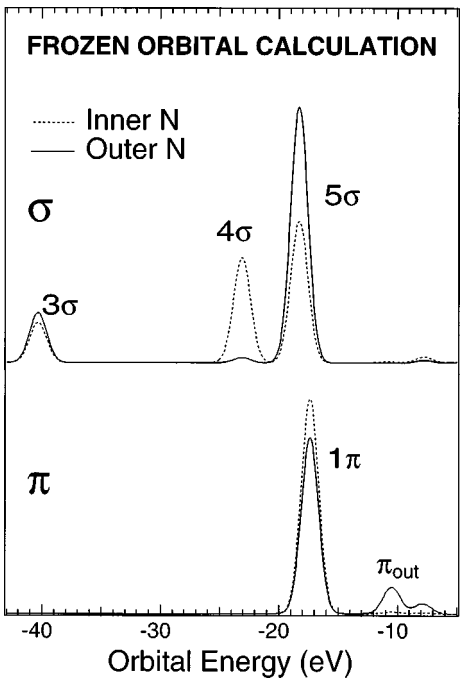

FIG. 5. Calculated XE spectra for N_2/Ni_{13}. Here the intensities are given by the explicit dipole transition matrix elements using the ground-state orbitals to describe the initial and final states of the XE process. The discrete orbital spectra are broadened by a Gaussian with a FWHM of 1.7 eV. The spectra have further been normalized so that the σ and π spectra have the same area on the inner and outer atoms, respectively.

B. Generation of theoretical spectra

The present implementation of the theoretical treatment of XE spectra is valid for a single-determinant SCF wave function, while for a more accurate description of the adsorbate-substrate interaction a more advanced, multiconfiguration (CASSCF) wave function is required. For this CASSCF wave function we will thus generate more qualitative spectra based on the p-populations as given by the Mulliken population analysis; this corresponds to the one-center approximation for an initial $1s$ core-hole state. In order to calibrate this approach we will compute full spectra for the SCF case, and compare with those obtained from the population analysis of the SCF wave function. The introduction of dynamical correlation, as in the MR-ACPF scheme based on the CASSCF orbitals, implies in principle a step away from the strict molecular-orbital interpretation of the wave function; here the orbitals are defined in terms of eigenvectors of the density matrix. Orbitals with high occupation numbers can still be identified with their CASSCF counterparts, and we will use the comparison between the CASSCF populations and those obtained at the correlated level to discuss trends obtained from higher level calculations, i.e., whether introduction of dynamical correlation increases or decreases the population on a center in a particular orbital. In the present section we will focus on the calibration of the one-center, population-based spectrum interpretation with the full calculation of the spectra. The computed XE spectrum from the SCF wave function and the corresponding spectrum based on the one-center approximation (SCF orbitals) Mulliken p populations are compared in Figs. 5 and 6.

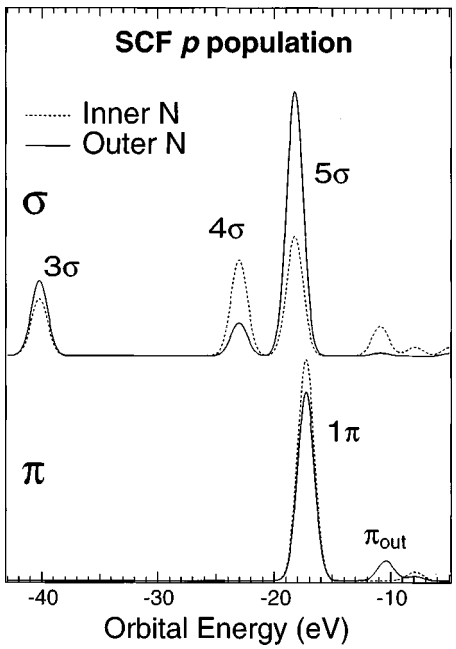

FIG. 6. Calculated Hartree-Fock SCF atomic Mulliken p_π and p_σ populations for the system N_2/Ni_{13}. The intensities are here given by the respective p populations on each molecular orbital. The discrete orbital spectra are broadened by a Gaussian with a FWHM of 1.7 eV.

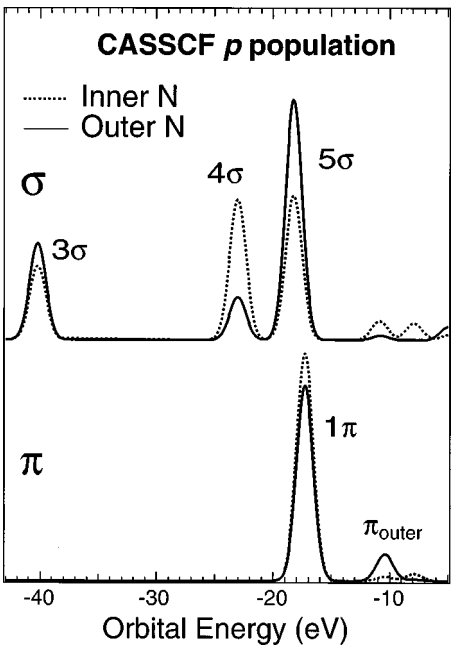

FIG. 7. Calculated CASSCF atomic Mulliken p_π and p_σ populations for the system N_2/Ni_{13}. The orbital energies were taken from the SCF calculation. Intensities are here given by the respective p populations for each molecular orbital. The discrete orbital spectra are broadened by a Gaussian with a FWHM of 1.7 eV.

It should be noted that the computed spectrum was generated within a ground-state, or frozen-orbital, picture to facilitate the comparison with the population-based spectra, which were generated from the ground-state populations. In the latter case the p populations on each nitrogen were simply read off from the list of Mulliken populations, convoluted with a Gaussian of FWHM 1.7 eV, and plotted against the orbital energies on a binding-energy scale. All peaks were normalized such that the highest peak had unit intensity. Comparing the thus-generated spectra, we find that the one-center approximation as an interpretation of the spectra holds very well in spite of the quite extended basis sets used in the present work. In the 4σ orbital the p population on the outer nitrogen is 0.11, where the sign indicates that it results mainly from antibonding combinations with other functions in the orbital, and has the character of an overlap population. This does not convert into an intensity in the full calculation of the spectrum, and should thus be ignored in discussing the contributions to the spectrum for the CASSCF wave function. Similarly the small populations on the inner nitrogen at 11 and 8 eV mainly have contributions from the diffuse part of the p basis, and do not show up in the explicitly computed spectrum. The peak at 4.9 eV, which shows up weakly on each nitrogen in the population spectrum, but not in the computed spectrum, can be traced to overlap populations, and will be discounted.

In the π symmetry the 1π and the weak peak (population 0.09 on the outer nitrogen) at 10.4 eV are accurately reproduced, while the smaller feature at 7.9 eV (populations 0.04 and 0.02 for inner and outer nitrogen, respectively) is only seen in the computed spectrum for the outer atom. All in all, the one-center approximation based on the population analysis seems to work quite well in reproducing the features of the XE spectra.

From the CASSCF calculation, we can now derive the p populations which are displayed in the form of a synthetic spectrum in Fig. 7. In order to obtain a more quantitative picture of the population analysis from both the SCF and CASSCF calculations, the result are also summarized in Table I.

C. CSOV analysis

In order to determine the different contributions to the bonding we have decomposed the total interaction energy according to the constrained space orbital variation (CSOV) (Refs. 37 and 38) scheme. Here the wave function for the noninteracting units (N_2 and cluster) is determined, after which the adsorbate is placed at the optimized geometry on

TABLE I. Mulliken population analysis.

Calculation	Orbital	N_{in} p	N_{out} p	N_{in} s	N_{out} s	Ni d
SCF	3σ	-0.193	-0.262	-0.703	-0.769	0.006
	4σ	-0.331	0.122	-1.156	-0.606	-0.065
	5σ	-0.368	-0.888	-0.196	-0.552	-0.034
	1π	-1.010	-0.880	-	-	-0.049
	π_{outer}	-0.003	-0.085	-	-	-1.809
	π_{in}	-0.039	-0.015	-	-	-0.025
CASSCF	3σ	-0.188	-0.247	-0.737	-0.750	0.006
	4σ	-0.358	0.110	-1.128	-0.608	-0.003
	5σ	-0.362	-0.880	-0.171	-0.614	0.000
	1π	-1.036	-0.892	-	-	-0.014
	π_{outer}	-0.018	-0.118	-	-	-1.677
	π_{in}	-0.032	-0.006	-	-	0.000

the cluster. The original wave function is kept frozen, except for orthogonality of the orbitals of the combined system, and the energy is computed for this initial, frozen system. The different interactions (substrate and adsorbate polarization, charge transfer, etc.) are then introduced stepwise, and the interaction energy is thus separated into the different contributions. The procedure is not well defined for correlated wave functions, and we will thus perform the analysis for the SCF wave function only, with the caveat that the system is unbound at this level; however, since we find quite substantial initial repulsion and polarization effects, it will still be of interest to analyze the origin of these.

The initial repulsion between the adsorbate and substrate with their frozen noninteracting wave functions is quite substantial, 4.73 eV, with the main origin of the repulsion in the σ space. When the adsorbate and cluster σ orbitals (a_1 orbitals in C_{2v} symmetry) are allowed to relax, the energy gain is 3.67 eV, which still leaves the molecule unbound by somewhat more than 1 eV. The π system (cluster and adsorbate) only contributes 0.49 eV to reduce the repulsion, which leaves a 0.05-eV contribution remaining in the fully relaxed binding energy of -0.52 eV (where the negative sign reflects the fact that at this level of calculation the molecule is not bound to the surface).

VI. DISCUSSION

The general trends in the spectra are well reproduced by the calculations. The different features in the spectra will be assigned to orbital characters from transition moment calculations and Mulliken population analysis. In the XES experiment, with an initial $1s$ hole state, only the p population can be measured, while the s populations remain undetected. We therefore mainly use the population analysis (see Table I) in our discussion of orbital characters. We will also use the wave functions of the DFT calculation, where more Ni atoms could be described at the all-electron level, for additional information. Based on our combined results, a model for the chemical bonding of chemisorbed N_2 on Ni(100) will be presented.

A. Orbital characters

The orbitals of interest are the N_2 valence orbitals, and the combinations that these make with the orbitals of the cluster, in particular the Ni $3d$. In the gas phase, for the free molecule, the molecular orbitals are symmetrically distributed between the two centers, but the interaction with the surface causes a polarization and reorganization of the orbitals. This reorganization involves not only the outermost, highest-energy orbitals, but the effects may be seen also on the chemically inert 3σ orbital which becomes slightly polarized toward the outer nitrogen. The effect is not large, but results in somewhat more p_z character on the outer atom than on the inner, as seen from Table I. The orbital is mainly dominated by $2s$ character, and the s populations are not affected. However, it is clear that even the deep-lying 3σ orbital is slightly perturbed through the interaction with the substrate.

In the σ manifold, the slightly antibonding 4σ orbital polarizes in the opposite sense from the 3σ, and about three times as much p character is found on the inner nitrogen. The population on the outer nitrogen is due to overlap with the other centers (Sec. V B) since the transition moment calculation shows only a negligible contribution, in accordance with the experiment. From the calculations we find a factor of 2 higher s population on the inner nitrogen, indicating that the s contribution to the orbital also polarizes to the inner atom, but much less so than the p contribution. Even though the orbital strongly polarizes toward the inner atom, it is clear that it is still a molecular orbital, and that it is mainly the p contribution that polarizes toward the inner nitrogen. The internally bonding 5σ orbital of chemisorbed N_2 contains mainly p character, with most of it located on the outer atom. In this case the total s population is lower, and shows an even larger asymmetry. There is no contribution of Ni character in any of the σ orbitals, indicating no direct overlap with the substrate, only an internal polarization of the orbitals. At a somewhat lower binding energy we find three orbitals with small N p contributions which do not possess any appreciable intensity in the transition moment calculation due to their rather diffuse character.

The 1π orbital is found in a (formally) *bonding* combination with the Ni $3d_\pi$ orbital, but the $3d$ contribution is low (0.01) at this level of calculation. Interestingly, when dynamical correlation is introduced through the MR-ACPF procedure, the contribution from $3d$ is found to increase to about 0.1 electrons in this bonding π orbital. The asymmetry within the nitrogen molecule is similarly increased from 1.04 (inner) and 0.89 (outer) to 1.02 and 0.77, respectively. Thus a result of the dynamical correlation is a slight charge transfer from the π-orbital to the $3d$ orbital in a bonding combination. The main $3d_\pi$ contribution is found in the interaction with the orbital that is traditionally denoted $\pi^\star$, which we find to be a basically *nonbonding* combination with very little weight on the inner nitrogen atom, and about 0.1 electron on the outer. This trend is again strengthened as a result of introducing a dynamical correlation, and an additional 0.1 electron is transferred from the $3d$ to the *outer* nitrogen. In the higher molecular orbitals we find small p contributions, mainly on the inner nitrogen. However, the transition moments for these orbitals are still higher on the outer nitrogen atom. This is the only discrepancy with the experiment, where the intensity for the orbitals close to the Fermi level is seen in both the inner and outer nitrogen spectra. The wave function in the DFT calculation provides some extra insight; the Ni $3d$ contributions to the 1π orbital and the nonbonding outer nitrogen π orbital are well reproduced. Since there are five all-electron Ni atoms included in the DFT calculation, the Ni $3d$ states become spread over a number of orbitals, showing the development of a d band. The outer nitrogen nonbonding contributions are spread over the main part of the Ni $3d$ ''band.'' The highest orbitals in the DFT calculation show an indication of a small $2p$ contribution on the inner nitrogen atom in an antibonding phase with the outer nitrogen atom. We could view this effect as a contribution of $\pi^\star$ character in the orbitals close to the Fermi level.

We cannot rule out that the experimentally observed intensity close to the Fermi level from the inner nitrogen can be related to core-hole-induced effects. We expect a larger

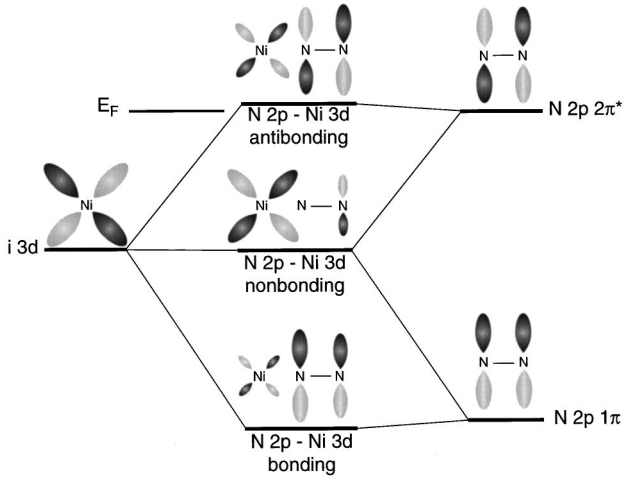

FIG. 8. Schematic illustration of the N_2 1π – Ni $3d$ interaction in terms of the atomic N $2p_\pi$ and Ni $3d_\pi$ orbitals.

modification of intensities between a computed frozen ground state and a relaxed core-hole state for final states close to the Fermi level.[8,39]

The calculations provide some further information about the unoccupied orbitals above the Fermi level. There is a $\pi^\star$ virtual orbital with an equal contribution of Ni $3d$, Ni $4p$, and N $2p$ which is antibonding between Ni and the molecule. This orbital has been observed in inverse photoemission of N_2 on Ni(100) at 4.5 eV above the Fermi level.[40]

Our results show that both the 1π and $2\pi^\star$ receive some contribution from Ni $3d$. It is interesting to compare with the isoelectronic CO adsorption system. An XAS study of CO on Ni(100) chemisorbed at the on-top site showed that there is a large contribution of Ni $3d$ character in the empty $2\pi^\star$ level,[41] which is different from the conclusions of Ref. 16, where an interaction with the Ni $4sp$ band was assumed. Furthermore, a high-energy excited valence-band photoemission spectrum showed an enhanced intensity of the 1π orbital relative to the σ orbitals.[42] This was related to a contribution from Ni $3d$, which has a much higher atomic photoemission cross section than C and O $2p$.

B. Surface chemical bond

From our results we can derive a model of the surface chemical bond which is different from the traditional Blyholder model. Instead of a σ donation, we show that the main effect from the σ system is a repulsive interaction. The π interaction cannot be explained only by considering a backdonation into the $2\pi^\star$ level. In order to create adsorbate orbitals, we need to involve the whole original π system of the free molecule, *i.e.*, both the 1π and $2\pi^*$ orbitals.

Figure 8 shows, in a simple MO picture, the interaction of the π system with the Ni $3d$. If we only consider the Ni atom which is directly involved in the bonding, the π system will involve three atoms, and three π orbitals will thus be generated in an allylic configuration.[43] The lowest orbital will (quite generally) always be bonding between all three centers, and the highest orbital will be antibonding. The intermediate orbital should be antibonding between the end atoms. In the case of a symmetric molecule, such as CO_2, there is no contribution on the center atom and this orbital can be denoted nonbonding. However, in an asymmetric molecule there could be a contribution from the center atom, and the orbital would become bonding and antibonding with respect to the different end atoms. In our case we can see, from the discussion in Sec. VI A, that this simple picture is consistent, and three different π orbitals are generated, as shown in Fig. 8. The bonding orbital is similar to the free molecule 1π orbital, only slightly polarized on the inner nitrogen atom with a small but significant contribution from the Ni $3d$ orbital. Since the 1π population is smaller compared with the free molecule, we have weakened the N-N bond and instead formed a (weak) covalent Ni-N interaction. The intermediate orbital is essentially nonbonding with a main contribution from the metal. The antibonding orbital is unoccupied, and the molecular character is similar to the $2\pi^\star$ orbital of the free molecule, with major contributions from the Ni $3d$ and $4p$ orbitals. This orbital structure was previously discussed in cases of simple metal dinitrogen and carbonyls compounds involving only one molecular ligand.[44,45,43]

For the real surface, these three orbitals will undergo changes due to the interaction with extended states in the metal. In order to keep the picture simple, we can envisage that each level becomes broadened with the bandwidth of the interacting substrate states.[46,47] Since the contribution of Ni $3d$ in the bonding orbital is rather small, the width will be governed by the discrete molecular 1π level. The nonbonding orbital is dominated by the Ni $3d$ orbital, and in this case we can anticipate a broadening with the width of the Ni $3d$ band. From Fig. 3 we can estimate the FWHM to 3 eV, which is close to the FWHM of the Ni $3d$ band in the bulk. The antibonding state will be even further broadened through the interaction with both Ni $3d$ and $4p$. In particular, the bandwidth of Ni $4p$ is much larger than the $3d$-bandwidth. Through this broadening the three levels will partly overlap each other. This can be seen in the continuous distribution between the bonding and nonbonding states in Fig. 3. Since the antibonding states are broadened to a much larger extent, we can easily envisage a small tail extending all the way down to the Fermi level, where it starts to overlap with the nonbonding states. In this case we will also see a small contribution on the inner nitrogen atom in the nonbonding states, as seen in the small structure close to the Fermi level in the inner nitrogen spectrum in Fig. 3.

In the interaction with the surface the nitrogen σ system will experience a repulsion against the $4sp$ orbitals of the cluster; this repulsion must be reduced in order for the molecule to approach closely enough to form a bond to the surface. In the interaction with a single nickel atom there are only two possibilities to reduce the repulsion: either through an s-d hybridization[20] or through the formation of a $4sp$ polarized orbital, where the s-d hybridization is energetically more favorable. At the surface it becomes instead even more favorable to polarize the central $4sp$ density out toward the surrounding metal centers, and this is the solution we find to be energetically more stable in the calculations. We find the Ni atom to be in a d^9 state, where the $4s$ electron has been polarized out on the cluster.

The repulsion can be understood in more detail from the CSOV decomposition of the interaction energies (cf. Sec. V C). As the N_2 is brought close to the surface, the large

Pauli repulsion is mainly relieved through a polarization of the $4sp$ density from the central Ni atom; this is also indicated in the population analysis as a loss of the $4s$ electron leading to a higher charge by about half a unit charge on the central Ni atom compared to in the naked cluster. As a result of this, we see a stabilization of the 4σ and 5σ levels through the interaction with the less screened Ni nuclear charge; the 4σ is stabilized by 1.6 eV, and the 5σ by 1 eV. Thus the polarization of the substrate allows a dative-type stabilizing interaction[48] between mainly the N_2 4σ lone pair and the substrate. There is an additional stabilizing effect seen from the polarization of the adsorbate, which can be viewed as a reduction of the antibonding character of the 4σ orbital. This is seen as a slight bond shortening, and an increase of the internal N-N vibrational frequency when only the σ interactions are included in the wave function.

To summarize the interactions in the σ system the dominating interaction is the Pauli repulsion between the adsorbate and the substrate $4sp$ charge density. As this is relieved through the polarization of the substrate, the adsorbate σ levels become electrostatically stabilized through interaction with the nuclear charge of the nearest Ni atom; we see very little involvement from Ni in these orbitals. Finally, the polarization of the 4σ orbital toward the substrate allows a reduction of the internal antibonding character, and results in a strengthening of the N-N bond, even though the 5σ bonding orbital polarizes the opposite way and some bonding character is thus lost. The reason that it is the 4σ and not the 5σ that polarizes toward the surface is probably due to the larger spatial extent of the 5σ, which would result in an even larger repulsion against the substrate.

The main part of the bonding occurs through the interaction of the 1π orbital with the Ni d band, with a partial split-off of a nonbonding lone pair state on the outer atom. This picture does not include any direct bonding involving the basically unperturbed $2\pi^\star$ level as in the usual pictorial description of the Blyholder model. However, the $2\pi^\star$ orbital contributes to the modification of the bonding 1π level and the formation of the nonbonding intermediate level (Fig. 8). In addition, it is present as a virtual, unoccupied level in the SCF and DFT calculations and as a correlating orbital (occupation 0.07 electrons) in the CASSCF calculations. In the latter case this orbital has a dual character, providing radial correlation for the $3d_\pi$ (i.e., it contains some formal $4d$ character) in addition to describing the $3d$-π interaction; the main part of the population in this orbital is actually of Ni d character with very small contributions from the N $2p$. Although this interaction is very important for the energetics, resulting in a slightly positive (0.3 eV) binding energy at this level compared with the -0.5 eV from the SCF wave function, we see only minor effects on the occupied levels.

The interpretation of the XE spectra in the recent short communication regarding the π states is thus slightly modified.[5] The two π states were interpreted as a N $2p$ lone pair state on the outer nitrogen atom and a local N $2p$–Ni $3d$ bonding state on the inner nitrogen atom. From the present work, we instead interpret the π state on the inner nitrogen atom as appearing due to an overlap of the nonbonding orbital with a contribution from the antibonding $2\pi^\star$ orbital. It was assumed in the previous paper that most of the bonding with the Ni $3d$ takes place through the inner atom π states. We now see that the main bonding contribution comes from the only slightly perturbed 1π orbital interacting with the Ni $3d$.

VII. CONCLUSIONS AND SUMMARY

In summary, by means of XES we have resolved the $2p$ contributions to the electronic structure for each of the two nitrogen atoms in the system N_2/Ni(100). The symmetry of the states, i.e., whether they have σ or π character, has also been determined. *Ab initio* calculations have been performed in order to provide further information on the atomic-orbital contributions to the surface chemical bond, as well as on the energetics in the bond formation.

The XE spectra show that the two nitrogen atoms contribute quite differently to the σ and π systems of the chemisorbed molecule, whereas in the gas phase the two atoms are equivalent. The σ system is found to redistribute compared to the gas phase, such that the $2p$ contributions to the 4σ orbital localize completely on the inner N atom, whereas the 5σ orbital is more located on the outer N atom. This is confirmed by the calculations, where it is also found that the $2s$ orbitals (which we do not probe in our experiment) also polarize in the same directions, but not to the same extent. The driving force for the redistribution is a Pauli repulsion between the N_2 σ system and the Ni $4sp$ bands. We note that the calculated results for the atomic-orbital populations for the σ system are in overall agreement with the results in the theoretical study by Hermann *et al.*[19] and Horn *et al.*[17] on NiN_2.

In the π system, basically three states are seen in the XE spectra: the 1π level, with intensity from both N atoms; and two states (compared to the gas-phase distribution) near the Fermi level with $2p$ contributions polarized to the outer and inner N atoms, respectively. These two orbitals are formed from the original 1π and $2\pi^*$ orbitals of the free molecule. Interestingly, it is found that there is some Ni $3d$ contribution in the ''1π'' level, and, from the analysis of our calculations, we find that all three states can be understood as the result of an N_2 1π–Ni $3d$ interaction. Furthermore, there is no sign in the calculations of any population of the gas phase N_2 $2\pi^\star$ corresponding to a donation from the nickel. This is in contradiction to the traditional Blyholder model, which is based on a σ donation combined with a backdonation into the π^* level. Instead, both from experiment and calculations, we see a partial breaking of the internal π bond with formation of a covalent 1π-$3d$ interaction between the inner nitrogen and the nickel combined with formation of a nonbonding lone-pair state on the outer nitrogen. The π^* level is mainly unoccupied, but is seen in the XE spectra as a small contribution at the Fermi level. Since this level interacts both with the $3d$ and $4sp$ bands, it becomes substantially broadened, with a small tail extending below the Fermi level into the occupied density of states.

In other words, we arrive at a picture of the surface chemical bond which is contradictory to the normal ''frontier orbital'' models: even for a system like N_2/Ni(100), with a rather small chemisorption energy, the effects on the molecule are still large enough that a picture where the molecule is treated as a unit based on the gas-phase molecular-orbital

structure is not meaningful. Instead, we believe that in order to understand all aspects of the surface chemical bond, one has to start from an atomic-orbital based view, as has become possible through the x-ray-emission spectroscopy discussed in the present work.

ACKNOWLEDGMENTS

This research was supported by the Swedish Natural Science Research Council (NFR) and by the Göran Gustafssons Foundation for Research in Natural Science and Medicine.

[1] N. Wassdahl, A. Nilsson, T. Wiell, H. Tillborg, L. C. Duda, J. H. Guo, N. Mårtensson, J. Nordgren, J. N. Andersen, and R. Nyholm, Phys. Rev. Lett. **69**, 812 (1992).

[2] H. Tillborg, A. Nilsson, T. Wiell, N. Wassdahl, N. Mårtensson, and J. Nordgren, Phys. Rev. B **47**, 16 464 (1993).

[3] T. Wiell, H. Tillborg, A. Nilsson, N. Wassdahl, N. Mårtensson, and J. Norgren, Surf. Sci. **304**, L451 (1994).

[4] A. Nilsson, P. Bennich, T. Wiell, N. Wassdahl, N. Mårtensson, J. Nordgren, O. Björneholm, and J. Stöhr, Phys. Rev. B **51**, 10 244 (1995).

[5] A. Nilsson, M. Weinelt, T. Wiell, P. Bennich, O. Karis, N. Wassdahl, J. Stöhr, and M. G. Samant, Phys. Rev. Lett. **78**, 2847 (1997).

[6] A. Nilsson, N. Wassdahl, M. Weinelt, O. Karis, T. Wiell, P. Bennich, J. Hasselström, A. Föhlisch, J. Stöhr, and M. Samant, Appl. Phys. A: Solids Surf. **65**, 147 (1997).

[7] In the x-ray-absorption process the linearly polarized incident light leads to $1s\rightarrow\sigma$ and $1s\rightarrow\pi$ transitions if the **E** vector is parallel or perpendicular to the molecular axis, respectively. The same symmetry rules also hold for the emitted x rays. However, since we do not analyze the polarization of the emitted x rays, symmetry information only comes from the fact that the **E** vector is always perpendicular to the direction of the emitted x rays. In the case of normal emission from N_2 adsorbed perpendicular to the surface we therefore probe transitions from the two degenerate π orbitals to the N 1 core hole, whereas in grazing emission transitions from one of the π orbitals and the σ orbital are seen.

[8] V. Carravetta, L. G. M. Pettersson, O. Vahtras, and H. A. Ågren, Surf. Sci. **369**, 146 (1996).

[9] G. Blyholder, J. Phys. Chem. **68**, 2772 (1964).

[10] J. Stöhr and R. Jaeger, Phys. Rev. B **26**, 4111 (1982).

[11] W. F. Egelhoff, Surf. Sci. **141**, L324 (1984).

[12] C. Allyn, T. Gustafsson, and E. Plummer, Chem. Phys. Lett. **47**, 127 (1979).

[13] S. Andersson and J. B. Pendry, Phys. Rev. Lett. **43**, 363 (1979).

[14] D. A. King, Surf. Sci. **9**, 375 (1968).

[15] J. Tracy, J. Chem. Phys. **56**, 2736 (1972).

[16] C. R. Brundle, P. S. Bagus, D. Menzel, and K. Hermann, Phys. Rev. B **24**, 7041 (1981).

[17] K. Horn, J. Dinardo, W. Eberhardt, H-J. Freund, and E. W. Plummer, Surf. Sci. **118**, 465 (1982).

[18] R. J. Smith, J. Anderson, and G. J. Lapeyre, Phys. Rev. B **22**, 632 (1980).

[19] K. Hermann, P. S. Bagus, C. R. Brundle, and D. Menzel, Phys. Rev. B **24**, 7025 (1981).

[20] P. Siegbahn and M. Blomberg, Chem. Phys. **87**, 189 (1984).

[21] C. M. Kao and R. P. Messmer, Phys. Rev. B **31**, 4835 (1985).

[22] A. Rives and R. Fenske, J. Chem. Phys. **75**, 1293 (1981).

[23] J. Nordgren, G. Bray, S. Cramm, R. Nyholm, J. E. Rubensson, and N. Wassdahl, Rev. Sci. Instrum. **60**, 1690 (1989).

[24] A. Nilsson, H. Tillborg, and N. Mårtensson, Phys. Rev. Lett. **67**, 1015 (1991).

[25] P. Widmark, P.-Å. Malmqvist, and B. Roos, Theor. Chim. Acta **77**, 291 (1990).

[26] A. Wachters, J. Chem. Phys. **52**, 1033 (1970).

[27] I. Panas, P. Siegbahn, and U. Wahlgren, Chem. Phys. **112**, 325 (1987).

[28] U. Wahlgren and P. Siegbahn, in *Metal-ligand Interactions: from Atoms, to Clusters, to Surfaces*, edited by D. Salahub (Kluwer, Dordrecht, 1991).

[29] A. St-Amant and D. Salahub, Chem. Phys. Lett. **169**, 387 (1990).

[30] D. R. Salahub, R. Fournier, P. Mlynarski, I. Papai, A. St-Amant and J. Ushio, in *Density Functional Methods in Chemistry*, edited by J. Labanowski and J. Andzelm (Springer, New York, 1991), p. 77; A. St-Amant, Ph. D. Thesis, Université de Montréal, 1992. The present version of the program was substantially modified by L. G. M. Pettersson.

[31] H. Tatewaki and S. Huzinaga, J. Chem. Phys. **71**, 4339 (1979).

[32] J. P. Perdew and Y. Wang, Phys. Rev. B **45**, 13 244 (1992); J. P. Perdew, in *Electronic Structure of Solids*, edited by P. Ziesche and H. Eischrig (Akademie Verlag, Berlin, 1991); J. P. Perdew, J. A. Chevary, S. H. Vosko, K. A. Jackson, M. R. Pederson, D. J. Singh, and C. Fiolhais, Phys. Rev. B **46**, 6671 (1992).

[33] J. Almlöf, K. Faegri, Jr., and K. Korsell, J. Chem. Soc. Chem. Commun. **3**, 385 (1982).

[34] H. Ågren, V. Carravetta, O. Vahtras, and L. Pettersson, Chem. Phys. Lett. **222**, 75 (1994).

[35] A. Sandell, O. Björneholm, A. Nilsson, E. O. F. Zdansky, H. Tillborg, J. N. Andersen, and N. Mårtensson, Phys. Rev. Lett. **70**, 2000 (1993).

[36] A. Nilsson, E. Zdansky, H. Tillborg, O. Björneholm, N. Mårtensson, J. N. Andersen, and R. Nyholm, Chem. Phys. Lett. **197**, 12 (1992).

[37] P. Bagus, K. Hermann, and C. Bauschlicher, J. Chem. Phys. **80**, 4378 (1984).

[38] P. Bagus, K. Hermann, and C. Bauschlicher, J. Chem. Phys. **81**, 1966 (1984).

[39] U. v. Barth and G. Grossmann, Phys. Rev. B **25**, 5150 (1982).

[40] P. D. Johnson and S. L. Hulbert, Phys. Rev. B **35**, 9427 (1987).

[41] B. Hernnäs, O. Björneholm, A. Nilsson, H. Tillborg, A. Sandell, N. Mårtensson, M. Karolewski, and J. N. Andersen, Phys. Rev. B **47**, 16 052 (1993).

[42] A. Nilsson and N. Mårtensson, Phys. Rev. B **40**, 10 249 (1989).

[43] D. L. Dubois and R. Hoffmann, Nouv. J. Chem. **1**, 479 (1977).

[44] T. A. Albright, J. K. Burdett and M-H. Whenghbo, *Orbital Interactions in Chemistry* (Wiley, New York, 1985).

[45] R. Hoffmann, M. M-L. Chen, and D. L. Thorn, Inorg. Chem. **16**, 503 (1977).

[46] P. W. Anderson, Phys. Rev. **124**, 42 (1961).

[47] D. M. Newns, Phys. Rev. **178**, 1123 (1969).

[48] P. S. Bagus and K. Hermann, Phys. Rev. B **33**, 2987 (1986).